Chinese Journal of
POLYMER SCIENCE

RESEARCH ARTICLE

https://doi.org/10.1007/s10118-025-3387-6
Chinese J. Polym. Sci. **2025**, *43*, 1690–1698

Segment Miscibility Variations Dominating Stereocomplex Crystallization in Polymer Blends with Different Initial Chain Conformations

Zi-Xiang Dai, Zi-Yue Gao, Xiao-Kai Ye, Jian-Long Wen, Yong-Qiang Ming, and Yi-Jing Nie*

Institute of Polymer Materials, School of Materials Science and Engineering, Jiangsu University, Zhenjiang 212013, China

Abstract Understanding the mechanisms that influence the formation of stereocomplex crystals (SCs) in poly(lactic acid) (PLA) is critical for achieving effective regulation of SC content. In the current simulations, we constructed polymer blends with different initial chain conformations and then obtained four groups of polymer blend systems with similar segment miscibility but different chain extension degrees by controlling the high-temperature relaxation time. The simulation results indicate that the fraction of SCs formed in these systems is closely correlated with the average mixing parameters during the crystallization process rather than the initial chain extension degrees. In other words, the average segment miscibility in the crystallization process is the key factor controlling the formation ability of SCs.

Keywords Monte Carlo simulation; Stereocomplex crystallization; Segment miscibility

Citation: Dai, Z. X.; Gao, Z. Y.; Ye, X. K.; Wen, J. L.; Ming, Y. Q.; Nie, Y. J. Segment miscibility variations dominating stereocomplex crystallization in polymer blends with different initial chain conformations. *Chinese J. Polym. Sci.* **2025**, *43*, 1690–1698.

INTRODUCTION

Currently, the world is paying increasing attention to the relationship between materials, environment, and resources.[1–3] Improper disposal of non-biodegradable plastics can cause serious environmental pollution.[4,5] In addition, the extensive use of non-renewable plastics can lead to continuous consumption and wastage of resources. In this situation, academia and industry are increasingly focusing on the research and promotion of new renewable and biodegradable materials, such as poly(lactic acid) (PLA).[6–8] The main raw materials for synthesizing PLA are plants, which are renewable. In addition, PLA materials can degrade into water and carbon dioxide in the environment. They also exhibit good biocompatibility.[8] Based on these advantages, experts continue to expand the applications of PLA, such as its use in food packaging, bio-based plasticizers, textiles, drug delivery systems, and 3D/4D printing materials.[1–5,9–11] However, PLA has the disadvantages of weak mechanical properties and poor heat resistance, and its large-scale application is limited.[12] Then, various methods have been proposed to improve the mechanical properties and thermal stability of PLA.[13,14]

An effective method for improving the mechanical properties and thermal stability of PLA is to increase the content of stereocomplex crystals (SCs) that form between the poly(L-lactic acid) (PLLA) and poly(D-lactic acid) (PDLA) chains during crystallization.[7,15,16] In 1987, Ikada *et al.* first observed the formation of SCs between PLLA and PDLA chains.[17] Zhang *et al.* found that in PLLA/PDLA blends, hydrogen bonds could be formed between the PLLA and PDLA segments, promoting the formation of SCs.[18] Compared to homocrystals (HCs) formed in pure PLLA or PDLA, SCs have a higher melting point, and PLA materials containing more SCs usually exhibit stronger mechanical strength.[15,16] There are many research works focusing on how to improve the SC content and optimize the PLA performance by increasing the SC content.[7,19–23]

It should be noted that there are many factors that affect the formation of SCs, such as segmental mobility, segment miscibility, chain-folding ability, and supercooling degree for HC and SC formation, *etc.*[24–32] However, the factors that dominate the formation of SCs remain controversial. The challenge in studying the impacts of these factors on SC formation lies in their interdependence, as altering one factor can lead to changes in others. For instance, if two types of polymer chains are alternately grafted onto substrates, the chain conformation will be extended owing to the crowding effect of the grafted chains, thereby reducing the chain-folding ability.[33] In the meantime, the miscibility of segments belonging to different polymer chains increases.[33] Then, to ensure the isolation of variables and avoid confounding effects, it is essential to maintain all other factors constant when examining the influence of a specific factor on SC formation. Compared with experiments, it is more convenient to control the

* Corresponding author, E-mail: nieyijing@ujs.edu.cn

Received April 30, 2025; Accepted May 21, 2025; Published online July 18, 2025

corresponding parameters in simulations.[29,31,33–35] Hu *et al.* applied dynamic Monte Carlo (MC) simulations to study the stereocomplex crystallization of polymer blends for the first time.[36] They demonstrated that intermolecular interactions play a dominant role in the formation of polymer-staggered crystals (SCs).[36] Our group established polymer blend systems with different segment miscibilities by setting different diffusion time.[33] Then, the effects of other factors, such as segmental mobility, chain-folding ability, and supercooling degree, on HC and SC formation can be excluded. It was demonstrated that the segmental miscibility of the two enantiomers plays a key role in the formation of SCs.[33] More and more experimental results have also confirmed that miscibility between PLLA and PDLA segments affects the formation process of SCs.[28,37–39]

To further confirm that the influence of segment miscibility on SC formation is the most significant, we constructed polymer blend systems with varying degrees of initial chain extension. Subsequently, by adjusting the relaxation times of these polymer blend systems with varying degrees of initial chain extension, we obtained four groups of amorphous polymer blend systems with similar segment miscibility but different degrees of chain extension. Finally, the dependence of the SC formation ability of these systems on the degree of segment miscibility and chain extension was investigated. The simulation results demonstrated that SC formation ability is closely correlated with the average segment miscibility during crystallization rather than the initial chain extension degree, demonstrating that segment miscibility during crystallization is the dominant factor affecting SC formation.

SIMULATION DETAILS

The current MC simulations were carried out in the lattice space to ensure the efficiency of the simulations. First, we constructed a cube simulation box with 64 lattice sites in side length and placed two kinds of polymer chains with the same chain length (64 beads), labeled as A polymer chains and B polymer chains, respectively. A detailed description of the lattice space can be found in literature.[40] The A/B polymer chains consisted of 64 connected, coarse-grained beads. One of the characteristics of the current lattice space is that only one polymer bead can be located at one lattice site. To simulate the bulk polymer systems, the occupation density of the polymer beads was maintained at 0.9375. The number of A and B polymer chains accounted for half of the total number of chains. Four initial polymer blend systems containing chains with different degrees of chain extension were established, as shown in Fig. 1. In the first polymer blend system (system (a)), as shown in Fig. 1(a), each chain underwent three folds and was then placed into the simulation box along the *X*-axis direction. Thus, the length of each chain along the *X*-axis direction was 16 beads. In the second polymer blend system (system (b)), as shown in Fig. 1(b), each chain underwent one fold and was then placed into the box along the *X*-axis direction, and the length of each chain along the *X*-axis direction was 32 beads. In the third polymer blend system (system (c)), each chain was folded once and then placed in the box along the *X*-axis direction, as shown in Fig. 1(c). One part of each chain had a length of 48 beads along the *X*-axis direction, and the other part had a length of 16 beads along the *X*-axis direction (that is, the length of each chain along the *X*-axis direction was 48 beads). In the fourth polymer blend system (system (d)), all chains with extended chain conformation were directly introduced into the box, and the length of each chain along the *X*-axis direction was 64 beads, as shown in Fig. 1(d). Under these conditions, four polymer blend systems with different degrees of chain extension were obtained.

Hu *et al.* introduced a parallel interaction parameter (E_p) to drive the polymer crystallization process in dynamic MC simulations for the first time.[40,41] Considering the formation of intermolecular hydrogen bonds between adjacent PLLA segments and PDLA segments in SCs, the energy reduction caused by the parallel arrangement of one PLLA segment and one PDLA segment should be greater than that caused by the parallel arrangement of two PLLA segments or two PDLA segments. In other words, the E_p value corresponding to the energy reduction caused by the parallel packing of one PLLA segment and one PDLA segment should be higher than that corresponding to the energy reduction caused by the parallel

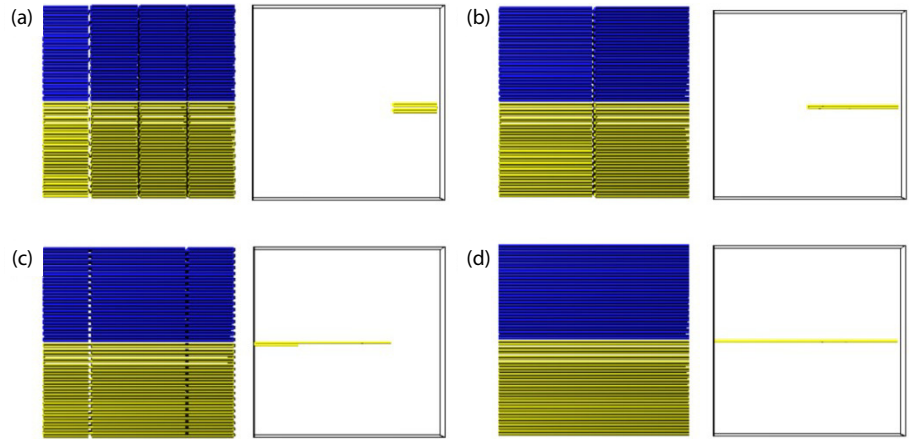

Fig. 1 Snapshots for the initial polymer blend systems with different chain conformations, that is, the polymer blend systems containing chains with the lengths of (a) 16 beads, (b) 32 beads, (c) 48 beads, and (d) 64 beads along the *X*-axis direction, respectively. The blue cylinders denote the segments belonging to the A polymer chains, and the yellow cylinders denote the segments belonging to the B polymer chains.

https://doi.org/10.1007/s10118-025-3387-6

packing of two PLLA or two PDLA segments.

Previous studies by Hu *et al.* demonstrated that assigning higher E_p values to the parallel stacking of different types of chain segments promotes stereocomplex crystallization in polymer blends.[36] Therefore, based on this pioneering simulation, we assigned distinct E_p values for the parallel stacking of different types of chain segments. During simulations, the chain motion followed a micro-relaxation mode that included the positional hopping of beads as well as the local slippage of chain segments, allowing polymer chains to flexibly adjust their conformation within the simulated space.[40] To further ensure the accuracy and reliability of the simulation results, we implemented periodic boundary conditions.

The movements of the chain segments during each MC cycle are governed by the Metropolis sampling algorithm.[40] This algorithm determines whether to accept a motion attempt based on the energy variation principle. In each MC cycle, every bead was granted an opportunity to attempt movement, enabling the polymer systems to evolve gradually over time. The number of MC cycles during the simulations was considered as a measure of simulation time. The potential energy change (ΔE) induced by the chain motion can be calculated as follows:

$$\frac{\Delta E}{kT} = \left[\Delta c + \Delta p_1 \frac{E_{p_1}}{E_c} + \Delta p_2 \frac{E_{p_2}}{E_c}\right] \frac{E_c}{kT} \quad (1)$$

where E_c is the change in potential energy caused by the formation of a non-collinear connection of two A or B polymer bonds and is related to the flexibility of polymer chains, E_{p_1} is the change in potential energy caused by the formation of a pair of non-parallel bonds of the same type (A polymer or B polymer) in adjacent regions, corresponding to the thermodynamic driving force of the HC formation, E_{p_2} is the change in potential energy caused by the formation of a pair of different types of non-parallel stacking bonds, corresponding to the thermodynamic driving force of the SC formation, Δc is the change in the number of non-parallel bond pairs, Δp_1 is the change in the number of A or B pairs that are non-parallel stacked, and Δp_2 is the change in the number of non-parallel stacked pairs that contain one A bond and one B bond. As mentioned above, different parallel interaction parameter values were set for the stacking of two A bonds or two B bonds ($E_{p_1}/E_c = 1$), and for the stacking of one A bond and one B bond ($E_{p_1}/E_c = 1.2$), as shown in Fig. 2. Previously, our group studied the SC formation mechanisms in different polymer blends based on the same parameter settings, including polymer blends with different chain lengths,[31] grafted polymer systems,[24,42] polymer blend systems filled with two-dimensional nanofillers,[43] polymer blend systems with different mixing degrees,[33] ring polymer systems[44,45] and block polymer systems.[25,46]

RESULTS AND DISCUSSION

Construction of Systems with Similar Initial Segment Miscibility but Different Degrees of Chain Extension

These four initially preset polymer blend systems were then relaxed under athermal conditions (that is, under an infinitely high temperature). Fig. 3(a) shows the changes in the crystallinity of these four polymer blend systems during the high-temperature relaxation process. Crystallinity is defined as the ratio of the number of crystalline bonds to the total number of polymer bonds (crystalline bond is defined as the bond that features more than five parallel bonds in its neighboring region).[25,31,33,36] The crystallinity in all four polymer blend systems decreases rapidly with increasing relaxation time, indicating that the crystals existing in these initially preset polymer systems melt rapidly during the relaxation process. The crystallinity values in all four polymer blend systems reached 0 after approximately 2000 MC cycles. That is, after 2000 MC cycles, all the polymer blend systems became polymer melts.

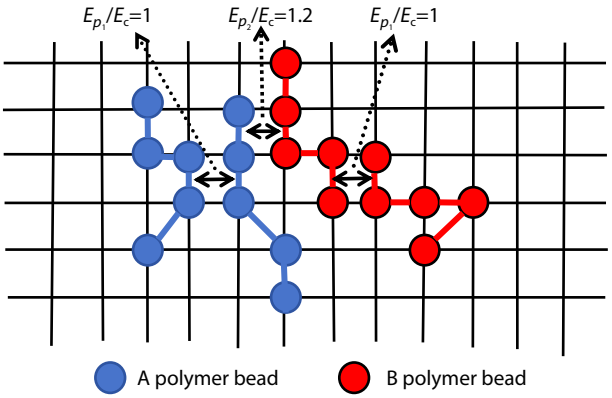

Fig. 2 Schematic diagram of the A and B coarse-grained chain segments and the setting of parallel interaction parameters between different bonds.

In addition to crystal melting, there are two other phenomena during the relaxation process: chain diffusion between the two different types of polymer chains and relaxation of the chain conformation. Fig. 3(b) shows the variations in the mixing parameters of the two types of polymer chains during the relaxation process. The mixing parameters were defined as the mean fraction of lattice sites occupied by one type of polymer chains in the neighboring regions of the other polymer chains.[31,45] With an increase in the relaxation time, the mixing parameters for all polymer blend systems first increase gradually and then level off, demonstrating that the two different polymer chains located on either side of the box undergo gradual diffusion and mixing during the relaxation process. In addition, the mixing parameters of these four polymer blend systems with different degrees of chain extension at the same relaxation time are almost the same, indicating that the diffusion rate of the chain segments or the mixing rate between the two polymer chains is dependent on the relaxation time rather than the degree of chain extension in the initially preset polymer systems.

Fig. 3(c) displays the changes in the mean square radius of gyration ($\langle R_g^2 \rangle$) of the chains in the four polymer blend systems during the relaxation process. For the three polymer systems containing chains of deformed conformation (system (b), system (c), and system (d)), the values of the $\langle R_g^2 \rangle$ for all the polymer blend systems decrease with increasing relaxation time, demonstrating that the deformed chains in these three systems relax to the random coil states to increase their conformation entropy.[47] For polymer systems containing chains without extension (system (a)), the values of the $\langle R_g^2 \rangle$ did not exhibit obvious changes.

Subsequently, by modulating the relaxation time, polymer

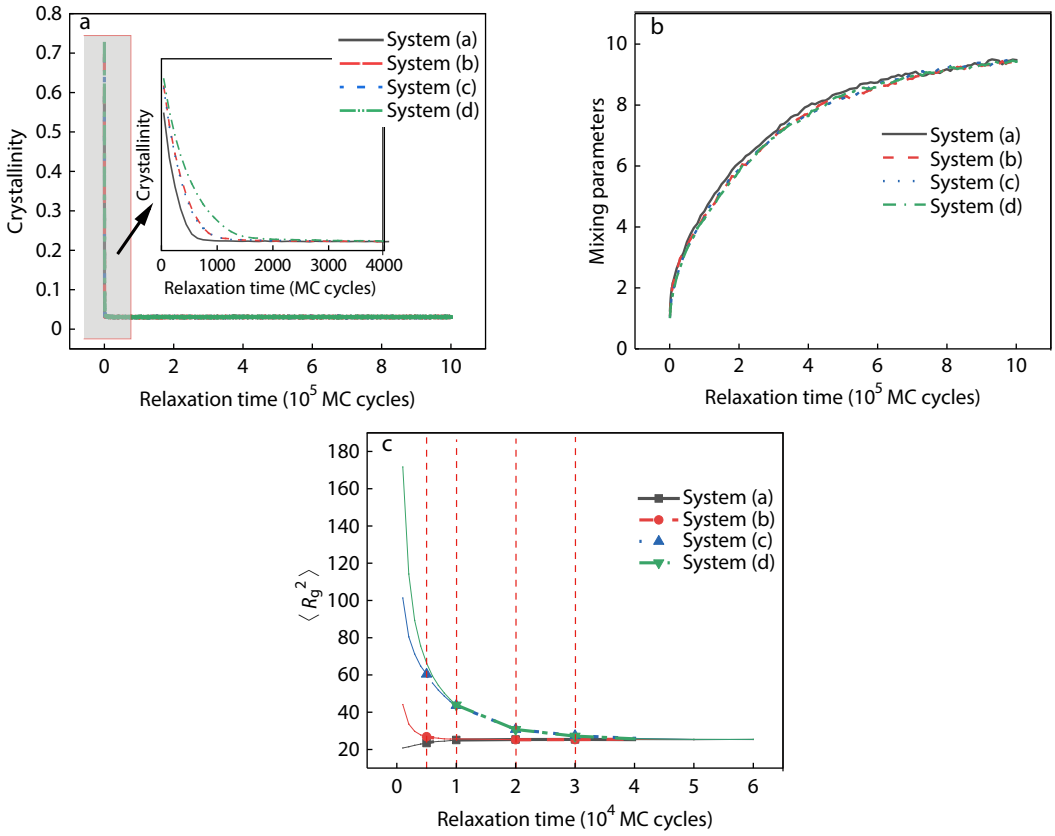

Fig. 3 (a) Evolutions of crystallinity of the four initially preset polymer blend systems during the relaxation process; (b) Evolutions of mixing parameters of the four initially preset polymer blend systems during the relaxation process; (c) Evolutions of mean square radius of gyration of chains in the four initially preset polymer blend systems during the relaxation process.

Table 1 Detailed information of the relaxed polymer blend systems with similar segment miscibility but different degrees of chain extension.

Relaxation time	System (a)/mixing parameter/$\langle R_g^2 \rangle$	System (b)/mixing parameter/$\langle R_g^2 \rangle$	System (c)/mixing parameter/$\langle R_g^2 \rangle$	System (d)/mixing parameter/$\langle R_g^2 \rangle$
5000 MC cycles	System (a)/0.071/23.44	System (b)/0.065/26.87	System (c)/0.061/60.44	System (d)/0.057/66.33
1×10^4 MC cycles	System (a)/0.082/25.08	System (b)/0.081/25.69	System (c)/0.071/43.62	System (d)/0.069/43.88
2×10^4 MC cycles	System (a)/0.100/25.35	System (b)/0.096/25.20	System (c)/0.088/30.76	System (d)/0.088/30.75
3×10^4 MC cycles	System (a)/0.111/25.37	System (b)/0.112/25.30	System (c)/0.102/27.43	System (d)/0.100/27.17

melt systems exhibiting different degrees of chain extension or different mixing parameters (segment miscibility) can be obtained. In the current simulations, four relaxation time (5000 MC cycles, 1×10^4 MC cycles, 2×10^4 MC cycles, and 3×10^4 MC cycles) were selected, and 16 polymer blend systems were obtained; the detailed information is displayed in Table 1. Systems with the same relaxation times have similar mixing parameters (*i.e.*, similar segment miscibility) but different chain extension degrees. Polymer blend systems with higher initial chain extension degrees before the relaxation process have higher chain extension degrees after certain relaxation times. However, with an increase in the relaxation time, the difference in the degrees of chain extension between the different systems decreases. When the relaxation time was 30000 MC cycles, there was little difference in the degrees of chain extension among the four polymer blend systems.

Isothermal Crystallization

Following the relaxation process, the 16 polymer blend systems were quenched to a specific low reduced temperature (kT/E_c = 3.0) for isothermal crystallization. The changes in the crystallinity values of the 16 polymer blend systems with different relaxation times during isothermal crystallization are displayed in Fig. 4. The crystallinity of all 16 polymer blend systems increased with increasing crystallization time, demonstrating that polymer crystallization occurred in all systems.

We then focused on SC formation in these 16 polymer blend systems. Based on the experimental results of the SC structures,[48] we defined the SC bond and the HC bond as follows: a crystalline bond is designated as a SC bond if the ratio of A-chain to B-chain crystalline bonds in the neighboring areas lies within 0.5–2; conversely, it becomes a HC bond when this ratio is not in this range.[24,25] The SC fraction was determined by dividing the number of SC bonds by the total number of crystalline bonds. Fig. 5 illustrates the morphologies of the SCs and HCs in the four polymer blend systems with a relaxation time of 5000 MC cycles after isothermal crystallization. Both the HCs with the local packing of crystalline bonds

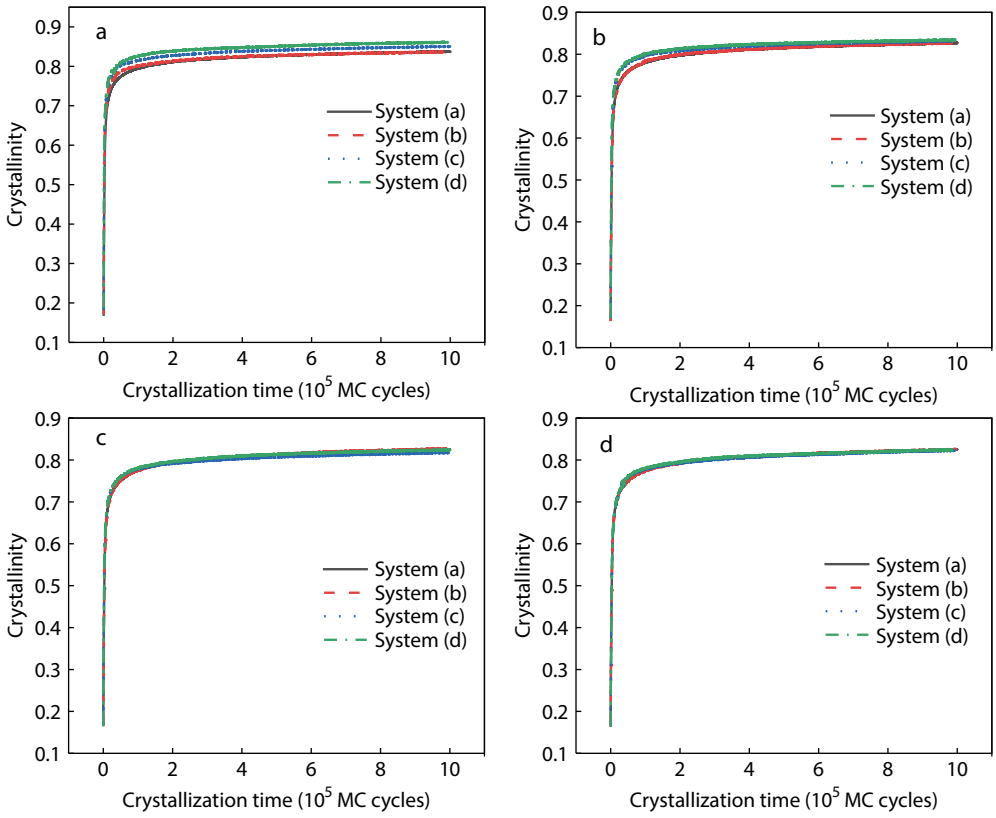

Fig. 4 Changes of crystallinity in the 16 polymer blend systems with different relaxation time, that is, (a) 5000 MC cycles, (b) 1×10^4 MC cycles, (c) 2×10^4 MC cycles and (d) 3×10^4 MC cycles during isothermal crystallization, respectively.

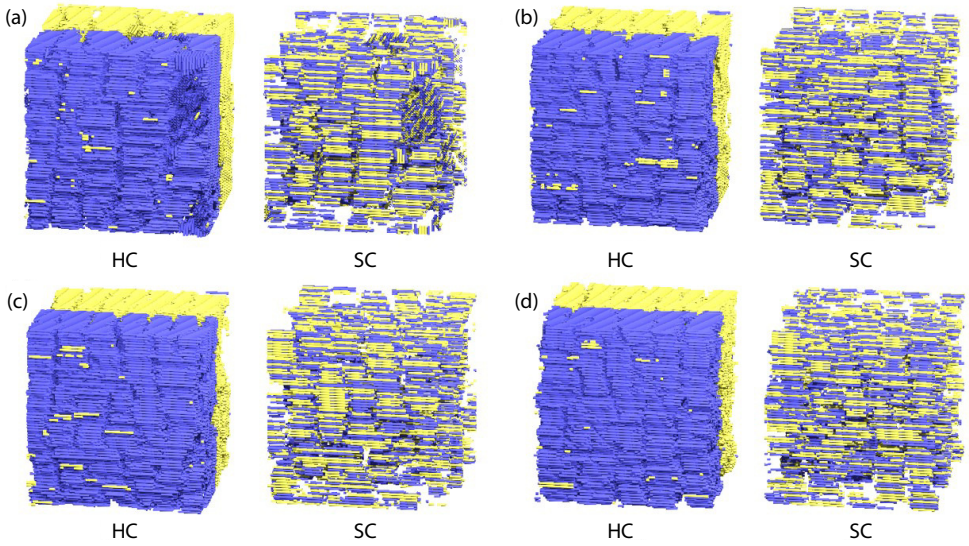

Fig. 5 Snapshots for the morphologies of HCs and SCs in (a) the crystallized system (a) with the relaxation time of 5000 MC cycles, (b) the crystallized system (b) with the relaxation time of 5000 MC cycles, (c) the crystallized system (c) with the relaxation time of 5000 MC cycles, and (d) the crystallized system (d) with the relaxation time of 5000 MC cycles. The blue cylinders denote the crystalline segments belonging to the A polymer chains, and the yellow cylinders denote the crystalline segments belonging to the B polymer chains.

belonging to the same type and the SCs with the local packing of crystalline bonds belonging to different types form in these systems.[31,37]

Fig. 6 displays the final SC fraction in the 16 polymer blend systems at the end of isothermal crystallization (10^6 MC cycles). As shown in Fig. 6, for the same polymer blend systems with different relaxation time, polymer blend systems with longer relaxation time exhibited higher final SC fractions. It should be noted that polymer blend systems with longer relaxation time have lower chain extension degrees (Fig. 3c and

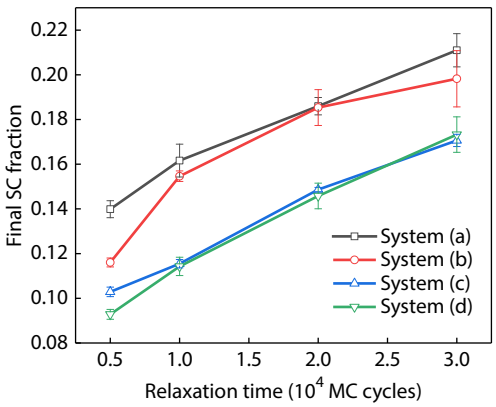

Fig. 6 Final SC fractions in the four polymer blend systems with different relaxation time.

Table 1). Thus, it can be concluded that the polymer blend systems with lower degrees of chain extension have a higher final SC fraction, which is somewhat inconsistent with the previous viewpoint, which assumes that polymer systems with a higher degree of chain extension would have higher SC content.[29,30] Overall, for these different polymer blend systems with the same relaxation time, polymer blend systems with lower initial chain extension degrees have higher final SC fractions. However, there were some exceptions. For example, at a relaxation time of 1×10^4 MC cycles, there is not much difference between the final SC fractions of systems (c) and (d). At a relaxation time of 2×10^4 MC cycles, the final SC fractions in systems (a) and (b) are almost the same, and the final SC fraction of system (c) is slightly higher than that of system (d). At a relaxation time of 3×10^4 MC cycles, the final SC fraction of system (d) was higher than that of system (c). These inconsistencies suggest the presence of other critical factors that determines the formation of SCs.

In our previous work, we demonstrated that local segmental miscibility is the key factor dominating the formation of stereocomplexes in polymer blends.[33,44] In the current work, it should be confirmed whether the SC formation in the polymer blend systems is also dominated by local segmental miscibility. Fig. 7 shows the variations in the mixing parameters of the four polymer blend systems with different relaxation time during isothermal crystallization. The mixing parameters in all four polymer blend systems with different relaxation time increased with an increase in the crystallization time during isothermal crystallization, demonstrating that the A and B polymer chains are mixed continuously during isothermal crystallization. For the polymer blend systems with relaxation time of 5000 MC cycles and 1×10^4 MC cycles, the systems with smaller initial chain extension degrees had higher mixing parameters under the same crystallization time. For the polymer blend systems with a relaxation time of 2×10^4 MC cycles, system (d) has the lowest mixing parameters during crystallization, followed by system (c). In the early stage of crystallization, the mixing parameters of system (a) are higher than those of system (b), but in the late stage of crystallization, the mixing parameters of system (b) are higher than those of sys-

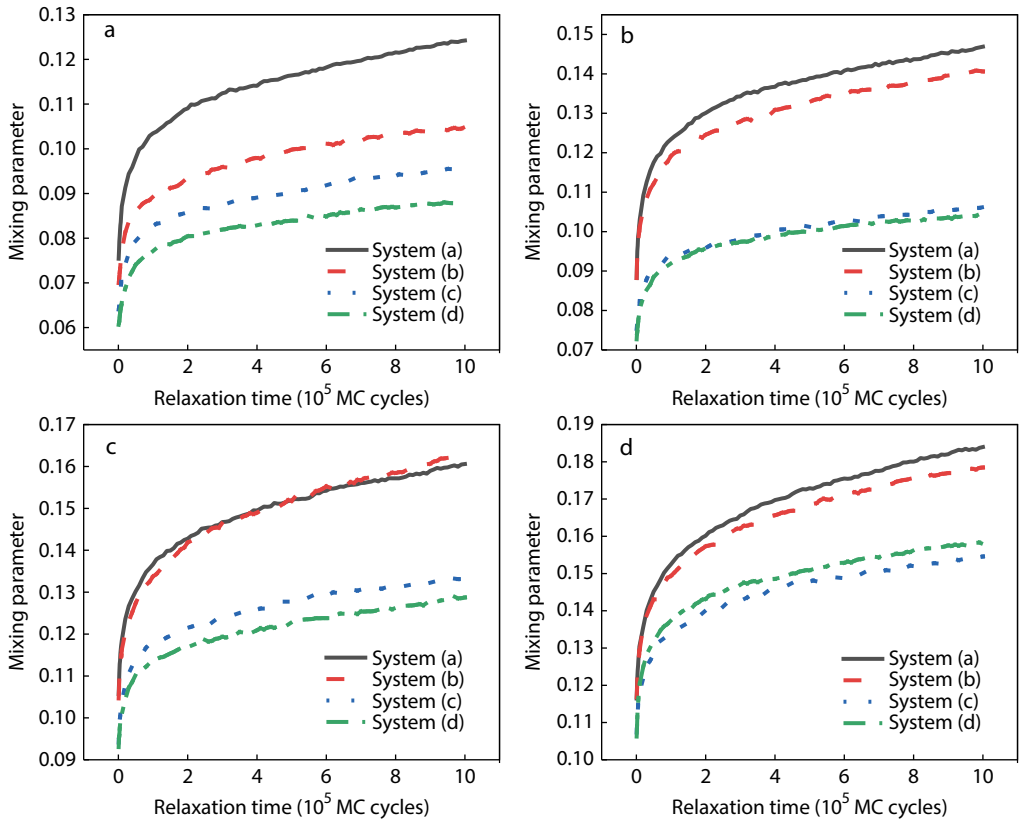

Fig. 7 Variations of the mixing parameters in all the four polymer blend systems with different relaxation time, that is, (a) 5000 MC cycles, (b) 1×10^4 MC cycles, (c) 2×10^4 MC cycles and (d) 3×10^4 MC cycles.

https://doi.org/10.1007/s10118-025-3387-6

tem (a). For the systems with a relaxation time of 3×10^4 MC cycles, system (a) had the highest mixing parameters during crystallization, followed by system (b), while system (d) had higher mixing parameters than system (c).

Based on the results in Figs. 6 and 7, it can be observed that the final SC contents and mixing parameters have a similar dependence on the relaxation time. We further attempted to confirm whether the final SC content has a close relationship with the mixing parameters. First, the average values of the mixing parameters of all polymer blend systems with different relaxation time during the crystallization process were calculated. Second, the final SC content was plotted versus the average mixing parameters, as shown in Fig. 8. It can be clearly seen that the final SC content increases with increasing average mixing parameters, implying that the SC formation ability is closely correlated with segment miscibility. To further verify the dependence of the SC formation ability on the segment miscibility, linear fitting was applied to the data in Fig. 8. It can be seen that there is a good linear relationship between the final SC fraction and the average mixing parameters, demonstrating that the SC formation ability closely depends on the segment miscibility.

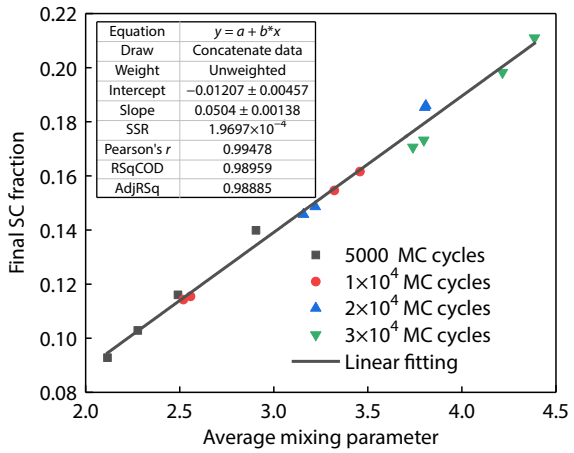

Fig. 8 The final SC fraction versus the average mixing parameters.

In short, the current simulation results demonstrate that local segment miscibility during the crystallization process plays a dominant role in the SC formation process, which is consistent with some reported experimental results. For instance, Hu *et al.* found that the effect of the correlation hole of neighboring monomers among high-molecular-weight polymers leads to a reduction in segmental miscibility, and thus hinders intermolecular nucleation for SC formation.[28] Lan *et al.* observed phase separation in high-molecular-weight PLLA/PDLA blends, which exerts a negative impact on SC formation.[37] The similar phase separation between PLLA and PDLA was also reported by Shi *et al.*[38]

The current new finding (that the average segment miscibility in the crystallization process is the key factor controlling the formation ability of SCs) can be used to guide the design of high-performance PLA materials. For instance, PLLA and PDLA chains can be chemically modified by introducing polar groups capable of forming hydrogen bonds. Then, the intermolecular interactions between the PLLA chains and the PDLA chains can be enhanced, leading to an improvement in the miscibility between the PLLA segments and the PDLA segments and an increase in the SC content. Thus, PLA materials with excellent mechanical properties can be obtained.

CONCLUSIONS

In this study, we investigated the effects of segment miscibility and chain extension on the formation ability of SCs. First, four polymer blend systems with different degrees of initial chain extension were constructed, and then these systems were relaxed at high temperatures. In the high-temperature relaxation process, the preset crystal melts, the chain conformation relaxes, and different types of chain segments are mixed with each other. The miscibility of segments of different types in these polymer blend systems is not related to the initial chain extensibility, but only to the high-temperature relaxation time. By controlling the high-temperature relaxation time, four groups of systems with similar mixing degrees but different degrees of chain extension were obtained. The SC formation abilities of these systems were studied. The final SC fraction in the systems with longer high-temperature relaxation time was higher. Further analysis showed that the final SC fractions in these systems had a linear relationship with the average mixing parameters during crystallization, demonstrating that the average segment miscibility in the crystallization process is the key factor controlling the formation ability of SCs.

Conflict of Interests

The authors declare no interest conflict.

Data Availability Statement

The associated data of this paper (DOI: 10.1007/s10118-025-3387-6) can be found at https://www.scidb.cn/c/cjps database https://www.scidb.cn/en/s/VFzilv.

ACKNOWLEDGMENTS

This study was financially supported by the National Natural Science Foundation of China (No. 52173020), the Qing Lan Project of Jiangsu Province of China (No. [2022]29) and the Jiangsu Provincial Science and Technology Plan Special Fund (No. BE2022128).

REFERENCES

1 Zhu, Y.; Romain, C.; Williams, C. K. Sustainable polymers from renewable resources. *Nature* **2016**, *540*, 354–362.
2 Liu, H.; Li, P. P.; Qiu, F. X.; Zhang, T.; Xu, J. C. Controllable preparation of FeOOH/CuO@WBC composite based on water bamboo cellulose applied for enhanced arsenic removal. *Food Bioprod. Process.* **2020**, *123*, 177–187.
3 Lu, Y.; Zhang, Y.; Zhang, K. Renewable biomass resources to access halogen-and phosphorus-free flame retardant thermosets with ultra-low heat release capacity. *Chem. Eng. J.* **2022**, *448*, 137670.

4 Khan, I.; Tariq, M.; Alabbosh, K. F.; Rehman, A.; Jalal, A.; Khan, A. A.; Farooq, M.; Li, G.; Iqbal, B.; Ahmad, N.; Khan, K. A.; Du, D. Soil microplastics: Impacts on greenhouse gasses emissions, carbon cycling, microbial diversity, and soil characteristics. *Appl. Soil Ecol.* **2024**, *197*, 105343.

5 Mangal, M.; Rao, C. V.; Banerjee, T. Bioplastic: an eco-friendly alternative to non-biodegradable plastic. *Polym. Inter.* **2023**, *72*, 984–996.

6 Swetha, T. A.; Ananthi, V.; Bora, A.; Sengottuvelan, N.; Ponnuchamy, K.; Muthusamy, G.; Arun, A. A review on biodegradable polylactic acid (PLA) production from fermentative food waste-its applications and degradation. *Inter. J. Biol. Macromol.* **2023**, *234*, 123703.

7 Bai, H.; Deng, S.; Bai, D.; Zhang, Q.; Fu, Q. Recent advances in processing of stereocomplex-type polylactide. *Macromol. Rapid Commun.* **2017**, *38*, 1700454.

8 Martin, O.; Avérous, L. Poly(lactic acid): plasticization and properties of biodegradable multiphase systems. *Polymer* **2001**, *42*, 6209–6219.

9 Sun, S.; Weng, Y; Zhang, C. Recent advancements in bio-based plasticizers for polylactic acid (PLA): a review. *Polym. Test.* **2024**, *140*, 108603.

10 Mehrpouya, M.; Vahabi, H.; Janbaz, S.; Darafsheh, A.; Mazur, T. R.; Ramakrishna, S. 4D printing of shape memory polylactic acid (PLA). *Polymer* **2021**, *230*, 124080.

11 Tyler, B.; Gullotti, D.; Mangraviti, A.; Utsuki, T.; Brem, H. Polylactic acid (PLA) controlled delivery carriers for biomedical applications. *Adv. Drug Deliv. Rev.* **2016**, *107*, 163–175.

12 Zhao, X.; Liu, J.; Li, J.; Liang, X.; Zhou, W.; Peng, S. Strategies and techniques for improving heat resistance and mechanical performances of poly(lactic acid) (PLA) biodegradable materials. *Inter. J. Biol. Macromol.* **2022**, *218*, 115–134.

13 Sharma, R.; Mehrotra, N.; Singh, I.; Pal, K. Development and characterization of PLA nanocomposites reinforced with bio-ceramic particles for orthognathic implants: Enhanced mechanical and biological properties. *Inter. J. Biol. Macromol.* **2024**, *282*, 136751.

14 Hughes, J.; Thomas, R.; Byun, Y.; Whiteside, S. Improved flexibility of thermally stable poly-lactic acid (PLA). *Carbohydr. Polym.* **2012**, *88*, 165–172.

15 Chen, Q.; Auras, R.; Uysal-Unalan, I. Role of stereocomplex in advancing mass transport and thermomechanical properties of polylactide. *Green Chem.* **2022**, *24*, 3416–3432.

16 Tan, B. H.; Muiruri, J. K.; Li, Z.; He, C. Recent progress in using stereocomplexation for enhancement of thermal and mechanical property of polylactide. *ACS Sustain. Chem. Eng.* **2016**, *4*, 5370–5391.

17 Ikada, Y.; Jamshidi, K.; Tsuji, H.; Hyon, S. H. Stereocomplex formation between enantiomeric poly(lactides). *Macromolecules* **1987**, *20*, 904–906.

18 Zhang, J.; Sato, H.; Tsuji, H.; Noda, I.; Ozaki, Y. Infrared spectroscopic study of CH_3···O=C interaction during poly(L-lactide)/poly(D-lactide) stereocomplex formation. *Macromolecules* **2005**, *38*, 1822–1828.

19 Zhang, Z. C.; Sang, Z. H.; Huang, Y. F.; Ru, J. F.; Zhong, G. J.; Ji, X.; Wang, R.; Li, Z. M. Enhanced heat deflection resistance *via* shear flow-induced stereocomplex crystallization of polylactide systems. *ACS Sustain. Chem. Eng.* **2017**, *5*, 1692–1703.

20 Xie, Q.; Guo, G.; Lu, W.; Sun, C.; Zhou, J.; Zheng, Y.; Shan, G.; Bao, Y.; Pan, P. Polymorphic homocrystallization and phase behavior of high-molecular-weight poly(L-lactic acid)/poly(D-lactic acid) racemic mixture with intentionally enhanced stereocomplexation ability *via* miscible blending. *Polymer* **2020**, *201*, 122597.

21 Michell, R. M.; Ladelta, V.; Da Silva, E.; Müller, A. J.; Hadjichristidis, N. Poly(lactic acid) stereocomplexes based molecular architectures: synthesis and crystallization. *Prog. Polym. Sci.* **2023**, *146*, 101742.

22 Diao, X.; Chen, X.; Deng, S.; Bai, H. Substantially enhanced stereocomplex crystallization of poly(L-lactide)/poly(D-lactide) blends by the formation of multi-arm stereo-block copolymers. *Crystals* **2022**, *12*, 210.

23 Yuan, L.; Deng, S.; Wang, Y.; Xiu, H.; Zhang, Q.; Bai, H. Remarkably enhanced stereocomplex crystallization of high-molar-mass enantiomeric polylactide blends by adding double-grafted copolymers. *Inter. J. Biol. Macromol.* **2024**, *258*, 128919.

24 Nie, Y.; Liu, Y.; Liu, R.; Zhou, Z.; Hao, T. Dynamic Monte Carlo simulations of competition in crystallization of mixed polymers grafted on a substrate. *J. Polym. Sci., Part B: Polym. Phys.* **2018**, *57*, 89–97.

25 Qiu, X.; Liu, R.; Nie, Y.; Liu, Y.; Liang, Z.; Yang, J.; Zhou, Z.; Hao, T. Monte Carlo simulations of stereocomplex formation in multiblock copolymers. *Phys. Chem. Chem. Phys.* **2019**, *21*, 13296–13303.

26 Pan, P.; Bao, J.; Han, L.; Xie, Q.; Shan, G.; Bao, Y. Stereocomplexation of high-molecular-weight enantiomeric poly(lactic acid)s enhanced by miscible polymer blending with hydrogen bond interactions. *Polymer* **2016**, *98*, 80–87.

27 Zhang, L. Q.; Zhang, Z. Y.; Yang, S. G.; Lei, J. Stereocomplex crystallization of equimolar poly(L-lactic acid)/poly(D-lactic acid) blends from melt with lowered chain entanglements. *Polymer* **2024**, *306*, 127229.

28 He, Y.; Liu, D.; Wang, J.; Pan, P.; Hu, W. Tammann analysis of the molecular weight selection of polymorphic crystal nucleation in symmetric racemic poly(lactic acid) blends. *Macromolecules* **2022**, *55*, 3661–3670.

29 Guan, X.; Wang, J.; Hu, W. Monte Carlo simulation of strain enhanced stereocomplex polymer crystallization. *J. Phys. Chem. B* **2018**, *122*, 10928–10933.

30 Xu, J. Z.; Li, Y.; Li, Y. K.; Chen, Y. W.; Wang, R.; Liu, G.; Liu, S. M.; Ni, H. W.; Li, Z. M. Shear-induced stereocomplex cylindrites in polylactic acid racemic blends: morphology control and interfacial performance. *Polymer* **2018**, *140*, 179–187.

31 Xu, Y.; Wu, H.; Yang, J.; Liu, R.; Zhou, Z.; Hao, T.; Nie, Y. Molecular simulations of microscopic mechanism of the effects of chain length on stereocomplex formation in polymer blends. *Comput. Mater. Sci.* **2020**, *172*, 109279.

32 Bao, R. Y.; Yang, W.; Wei, X. F.; Xie, B. H.; Yang, M. B. Enhanced formation of stereocomplex crystallites of high molecular weight poly(L-lactide)/poly(D-lactide) blends from melt by using poly(ethylene glycol). *ACS Sustain. Chem. Eng.* **2014**, *2*, 2301–2309.

33 Wen, J. L.; Ming, Y. Q.; Zhang, A. F.; Li, J. L.; Du, X. Y.; Shuai, L.; Nie, Y. J. Interplay between hydrogen bond network and entangled network in polymers during str*et*ching based on molecular simulations. *Chinese J. Polym. Sci.* **2024**, *42*, 2069–2080.

34 Zhou, Y. H.; Yang, J.; Zhou, Z. P.; Hao, T. F.; Nie, Y. J. Molecular dynamics simulations of str*et*ch-induced crystal changes in crystallized polyethylene/carbon nanotubes nanocomposites. *Chinese J. Polym. Sci.* **2023**, *41*, 1425–1438.

35 Zhu, Q.; Wen, J.; Ma, M.; Nie, Y. Local segmental miscibility dominating stereocomplex crystallization in polymer blends. *CrystEngComm* **2023**, *25*, 3885.

36 Zhang, R.; Zha, L.; Hu, W. Intramolecular crystal nucleation favored by polymer crystallization: Monte Carlo simulation evidence. *J. Phys. Chem. B* **2016**, *120*, 6754–6760.

37 Chen, Y.; Lan, Q. Experimental evidence for immiscibility of enantiomeric polymers: Phase separation of high-molecular-weight poly(L-lactide)/poly(D-lactide) blends and its impact on hindering stereocomplex crystallization. *Inter. J. Biol. Macromol.*

2024, *260*, 129459.
38 Chen, X.; Chen, G.; Shi, W. Polymer chirality modulates phase transitions at liquid-liquid interfaces. *Macromolecules* **2024**, *57*, 8851–8860.
39 Huang, Y.; Geng, D.; Ye, X.; Nie, Y.; Li, Z. Cooling rate guiding contradictory effect of thermal treated temperature on the crystallization of PLA racemic blends upon cooling. *Mater. Lett.* **2023**, *335*, 133708.
40 Hu, W. B.; Frenkel, D. Polymer crystallization driven by anisotropic interactions. In: Allegra G.(eds) *Interphases and Mesophases in Polymer Crystallization III*. Advances in Polymer Science, Book series vol. 191. Springer, Berlin, Heidelberg. **2025**, p. 1–35.
41 Nie, Y.; Zhao, Y.; Matsuba, G.; Hu, W. Shish-kebab crystallites initiated by shear fracture in bulk polymers: 2. Crystallization on shearing. *Polymer* **2023**, *274*, 125909.
42 Ma, J.; Chen, Y.; Chen, J.; Ming, Y.; Nie, Y. Molecular simulations of stereocomplex crystallization in grafted diblock copolymers. *Cryst. Res. Technol.* **2024**, *60*, 2400187.
43 Gu, Z.; Xu, Y.; Lu, Q.; Han, C.; Liu, R.; Zhou, Z.; Hao, T.; Nie, Y. Stereocomplex formation in mixed polymers filled with two dimensional nanofillers. *Phys. Chem. Chem. Phys.* **2019**, *21*, 6443–6452.
44 Zhu, Q.; Zhou, Z. P.; Hao, T. F.; Nie, Y. J. Significantly improved stereocomplexation ability in cyclic block copolymers. *Chin. J. Polym. Sci.* **2023**, *41*, 432–441.
45 Wu, H.; Wang, X.; Zhu, Q.; Yan, X.; Xue, Q.; Zhou, Z.; Hao, T.; Li, Z.; Nie, Y. Stereocomplex crystallization in cyclic polymer blends studied by dynamic Monte Carlo simulations. *CrystEngComm* **2023**, *25*, 1347–1357.
46 Xu, Y.; Yang, J.; Liu, Z. F.; Zhou, Z. P.; Liang, Z. P.; Hao, T. F.; Nie, Y. J. Stereocomplex crystallization in asymmetric diblock copolymers studied by dynamic Monte Carlo simulations. *Chinese J. Polym. Sci.* **2020**, *39*, 632–639.
47 Hu W. *Polymer Physics: A Molecular Approach*. Springer, Vienna. **2013**, p. 35.
48 Tashiro, K.; Kouno, N.; Wang, H.; Tsuji, H. Crystal structure of poly(lactic acid) stereocomplex: Random packing model of PDLA and PLLA chains as studied by X-ray diffraction analysis. *Macromolecules* **2017**, *50*, 8048–8065.

https://doi.org/10.1007/s10118-025-3387-6